Journal of Statistical Physics, Vol. 58, Nos. 3/4, 1990

Low-Concentration Series in General Dimension

Joan Adler,[1,2] Yigal Meir,[1] Amnon Aharony,[1] A. B. Harris,[1,3] and Lior Klein[1]

Received July 14, 1989

We discuss recent work on the development and analysis of low-concentration series. For many models, the recent breakthrough in the extremely efficient no-free-end method of series generation facilitates the derivation of 15th-order series for multiple moments in general dimension. The 15th-order series have been obtained for lattice animals, percolation, and the Edwards–Anderson Ising spin glass. In the latter cases multiple moments have been found. From complete graph tables through to 13th order, general dimension 13th-order series have been derived for the resistive susceptibility, the moments of the logarithms of the distribution of currents in resistor networks, and the average transmission coefficient in the quantum percolation problem. 11th-order series have been found for several other systems, including the crossover from animals to percolation, the full resistance distribution, nonlinear resistive susceptibility and current distribution in dilute resistor networks, diffusion on percolation clusters, the dilute Ising model, dilute antiferromagnet in a field, and random field Ising model and self-avoiding walks on percolation clusters. Series for the dilute spin-1/2 quantum Heisenberg ferromagnet are in the process of development. Analysis of these series gives estimates for critical thresholds, amplitude ratios, and critical exponents for all dimensions. Where comparisons are possible, our series results are in good agreement with both ε-expansion results near the upper critical dimension and with exact results (when available) in low dimensions, and are competitive with other numerical approaches in intermediate realistic dimensions.

KEY WORDS: Series expansion; percolation.

[1] School of Physics and Astronomy, Beverly and Raymond Sackler Faculty of Exact Sciences, Tel Aviv University, 69978 Tel Aviv, Israel.
[2] Department of Physics, Technion-HT, 32000 Haifa, Israel.
[3] Department of Physics, University of Pennsylvania, Philadelphia, Pennsylvania 19104.

0022-4715/90/0200-0511$06.00/0

1. INTRODUCTION

Professor C. Domb was a dominating force behind much of the groundbreaking work on the study of critical phenomena from exact series expansions. His major contributions in this problem include work on geometrical models such as percolation and lattice animals, and the development of the idea of using ratio methods to obtain critical exponents from the analysis of series. Excellent accounts of the early work can be found in Vols. 2 and 3 of the *Phase Transitions and Critical Phenomena* series[1,2] edited by Prof. Domb and the late Prof. M. S. Green. An introductory account of series for percolation processes was written by Professor Domb[3] for *Percolation Structures and Processes.* That article contains an excellent description of the parallels between concentration series for percolation and temperature expansions for the Ising model.

In the present paper we discuss the study of geometrical and other characteristics of disordered systems via multidimensional low-concentration series. This work extends Professor Domb's early efforts and thus we are happy to review this material for the volume in his honor. For reasons of space, we do not attempt to discuss thermal problems, high-concentration series, or dimension-specific methods of series generation (although Prof. Domb has recently worked on these problems). Emphasis is placed on those problems for which series for multiple moments are available in general dimension. A discussion of series generation methods and of the analysis methods that can be utilized efficiently when multiple moments are available is given in the next section. The final section contains a summery of recently published results for a variety of problems and some new exponent estimates for resistor networks.

The series expansion method is *in a sense* exact, as the aim is to write down the exact expansion of the quantity of interest (such as the free energy or one of its derivatives) as a series in increasing powers of some variable such as temperature T^{-1} (for magnetic systems) or concentration p (for percolation). This expansion is calculated on a term-by-term basis. The actual calculation is usually made by a computerized evaluation of the contributions from different graphs representing the different terms that contribute to the expansion up to some order in the variable T^{-1} or p. For example, the coefficients a_n in the expansion $\chi = \sum_n a_n p^n$ for the mean size χ of clusters of A atoms on a random alloy of A and B atoms are calculated by associating contributions to a_n with connected graphs consisting of n bonds. The numbers and types of these graphs are then enumerated to as high an order as possible, and the contribution from each is calculated and summed over. In its region of convergence the expansion would give us the exact solution if it could be carried to infinite order, but near the limit of

low (high) concentration an expansion in p ($q = 1 - p$) to a finite order will be quite reliable. When the expansion parameter is increased to some critical value, hereafter denoted as p_c, the quantity χ exhibits a singularity and we wish to use the series expansion to calculate p_c and the various critical exponents that describe the nature of this singularity. Here and below we emphasize the generality of these comments. In principle the quantity χ, and to a lesser extent the expansion parameter p, can be arbitrary, although the expansion for complicated quantities may be difficult to actually construct.

In practice, while the expansion does not take a closed form, series of over 50 terms for some problems and between 10 and 20 for many cases are not unusual nowadays, and enable accurate extrapolation into the critical region in order to obtain estimates of critical exponents or temperatures. This extrapolation involves determining the best fit to some proposed form for the singularity that the series can give. This is often done by calculating Padé approximants to some function derived from the singularity.

The early series work of Prof. Domb and his colleagues in the King's College group was carried out by hand. The first developments in the computerization of series generation are described by Martin,[4] and this work is especially remarkable in the context of the computer resources then available. The series expansion method, especially when efficient algorithms such as the no-free-end method[5,6] or the star-graph method[7] can be invoked, has an enormous future potential in the modern supercomputing environment. To date, only a small fraction of the computer resources that have been devoped to large-simulation[4] projects in critical phenomena have been applied to series generation. Despite this, series results are quite competitive with simulation estimates for nearly all problems.

Let us compare the series and simulation approaches, which are two of the most common numerical methods for obtaining solutions for models that exhibit critical phenomena. Simulations are usually made on the largest sample that is feasible, with extrapolation to the infinite system being required for application of the results. Statistical scattering of data can severely complicate the extrapolation, and a common scenario is that a great deal of computer time may fail to lead to accurate results. It is often the case that the problems are in the data analysis, but the nature of the calculations is such that it is often very difficult to store the simulation data in a compact from for future reanalysis. This is an important drawback because it prevents the kind of critical comparisons of results which

[4] See ref. 8 for an introduction to computer simulations, and ref. 9 for an introduction to simulation for percolation.

pervade the literature on series expansions. A related method involves solving the system exactly (by hand or by computer) for very small systems. This is equivalent to the series expansion technique, since the latter also involves an exact solution on finite graphs.

Both series and simulation calculations involve the two-stage process of data generation followed by data analysis. Data generation is usually the expensive part as far as computing resources are concerned. Data analysis is usually the more controversial stage of the project. Series have four great advantages over simulation. First, the most time-consuming effort, namely the enumeration of the graphs and the calculation of their weights, is done once only and can then be applied to many different problems. Calculation thereafter of the contribution of each graph to some averaged quantity is usually straightforward. Second, once different graphs are summed over, series data take an extremely compact form for storage, thus facilitating multiple analyses of each series. A single series calculation gives results expressed as a function of the expansion parameter, thereby summarizing the information for all possible choices of threshold value. Thus, the series method gives a real possibility of maximum utilization of all information. The third advantage is that because series is an enumeration rather than simulation approach, there are many built-in checks that can be applied to the data generation. Independent derivations that give exactly the same results strongly confirm the reliability of data, whereas statistical fluctuations complicate such cross-checks in the simulation case. The fourth advantage of the series method is specific to general-dimensional algorithms (a general-dimensional algorithm being one in which results are obtained as a general function, namely polynomial, of the spatial dimension d). These may be considerd to be highly parallelized calculations, in which all values of d are treated simultaneously, and as such represent an extremely efficient use of computer resources. To illustrate this point in a very extreme way, we point out that general d series up to 15th order for lattice animals for, say, $d=20$ give exact results, whereas simulations would require sampling a cluster population having in excess of 10^{20} elements. In this connection it should be noted that the time required in simulations of a given linear size of system increases drastically with increasing d. Beyond $d=4$ simulations are usually not competitive with series expansions (for the cases where the latter can be used). To balance these advantages, we note two disadvantages of series relative to simulations for certain problems. The first is that series systems are more limited in physical size, and thus may fail to allow for some features that are specific to larger systems. The second is that while efficient simulations give the best results/computer hour, relatively unsophisticated simulation algorithms can and have given many useful estimates for interesting

problems. Algorithms for the generation of series require, in general, a basic modicum of efficiency in order for any results to be obtained. This means that there is a certain startup time involved before series can become available for any new problem. Thus, the method of choice may depend on the requirements of the problem and it is probably best to use both approaches and compare the *independent* results, but it can be concluded that series represent an extremely efficient use of computer resources for a given problem.

2. SERIES GENERATION AND ANALYSIS

In this section we discuss the efficient generation and analysis methods that we have used for low-concentration and high-temperature problems in general dimension. There are many other approaches to series generation and analysis that we do not discuss in detail for reasons of space; some of these are presented in other articles in this volume. Some of the methods that have been applied for low-concentration models will be referenced in the next section when different systems are discussed.

For most problems one can generate series for any desired property χ via the expansion

$$\chi = \chi_0 + N \sum_{\Gamma} W(\Gamma)\, \chi_c(\Gamma) \tag{1}$$

where $W(\Gamma)$ is the number of times (per site) that the diagram Γ occurs on an infinite lattice and $\chi_c(\Gamma)$ is the cumulant value of χ calculated for the diagram Γ, defined recursively by

$$\chi_c(\Gamma) = \chi(\Gamma) - \sum_{\gamma \subset \Gamma} \chi_c(\Gamma) \tag{2}$$

χ_0 is the value of χ on the Cayley tree that has the same coordination number as the hypercubic lattice on which we wish to derive the series. In Eq. (2), $\gamma \subset \Gamma$ means that the sum is carried out over all diagrams γ which can be obtained from Γ by removing one or more bonds. In this formulation a diagram is a collection of bonds and $\chi_c(\Gamma)$ vanishes for all disconnected diagrams. One can interpret $\chi_c(\Gamma)$ as the contribution to χ which depends on all bonds in the diagram Γ. [Contributions to χ which depend on a subset γ of bonds of Γ were included in $\chi_c(\gamma)$ in a lower order.] We will consider several examples in which χ is a type of generalized susceptibility, i.e., of the form

$$\chi(p) = \left[\sum_j v_{ij} \chi_{ij} \right]_p \tag{3}$$

where $[\cdot]_p$ denotes configurational average, v_{ij} is unity if sites i and j are connected in a given configuration and zero otherwise, and χ_{ij} is some two-point function. The most important properties of $\chi_c(\Gamma)$ are (a) it vanishes if the diagram Γ is disconnected and (b) it depends on all n bonds in the diagram Γ. Therefore, the contribution of Γ to the sum in Eq. (1) is of nth order in the coupling constant p, T^{-1}, or any other perturbation away from a noninteracting problem. For most problems it is a simple task to evaluate the necessary $\chi(\Gamma)$'s. For example, to generate the high-temperature expansion for the susceptibility of the Ising model by this approach, one would have to evaluate $\chi(\Gamma)$, in this case the susceptibility, for all clusters having up to n bonds, where n is the desired order in p. Usually the limit on n is fixed by the need to tabulate the weak embedding constants $W(\Gamma)$ for all diagrams with up to n bonds. We have carried out[5,6] such tabulations for all diagrams with up to 13 bonds for the general d-dimension hypercubic lattices. Also, up to this order we have constructed a complete list of diagrams which can be embedded in a given diagram, in order to implement the recursive definition of the cumulant $\chi_c(\Gamma)$. The above information enables us to calculate the series expansion for any problem in which the property χ depends on the topology (but not the shape) of a given diagram. We will refer to this method as the "brute force" approach. In principle, one can evaluate series for properties which depend on the geometrical shape of the diagrams, but the required tabulation of diagrams is very time consuming.

For a wide class of problems we can simplify the above procedure. To do this, we eliminate from consideration all diagrams having one or more free ends. This is done by constructing the appropriate renormalized Hamiltonian as described in refs. 5 and 6. The renormalized Hamiltonian differs from the original Hamiltonian in that it includes a suitable site-dependent potential. For this procedure it is essential that the density matrix be expressible as the product of density matrices of individual bonds. Thus, this process is not applicable without severe modification to quantum systems. However, it can be applied in a straightforward way to replicated Hamiltonians which are used to describe various random problems. Usually the final renormalized Hamiltonian can be expressed without recourse to replica indices. (This is the case for the percolation and spin-glass problems described below.) We mention this lest the reader worry about the validity of the limit in which the number of replicas goes to zero. In this scheme, referred to as the "no-free-end (NFE) method," one carries the sum in Eq. (1) only over diagrams with no free ends. The price for this simplification is that one must deal with a renormalized Hamiltonian, but usually this represents dramatic savings in computational effort. (For 15 bonds, NFE diagrams represent about 0.1% of all

diagrams.) At present our list of weak embedding constants[6] of NFE diagrams consists of all diagrams (about 800 in number) with less than 16 bonds. This method has enabled the construction of many heretofore unmanageable series, some of which are described below.

Once the series has been generated, it must be analyzed. An early account of different methods of series analysis was given by Gaunt and Guttmann[10] and a more recent one by Guttmann.[11] Clearly, all the different methods of series generation must give the same result for each term of the series, since these are exact quantities. In contrast, different analysis methods give slightly different results, depending on the assumptions involved and the authors' weighting of different factors. When selecting a method for a particular series one must take into account variables such as the series length, the number of different series available in each dimension, and the expected contributions from analytic parts or from confluent singularities. One does not wish to have too many variable parameters for shorter series, and it is desirable to be able to utilize the redundancy that can be found from multiple moment series. (Here higher moments usually correspond to higher derivatives of the free energy with respect to a field at the critical point.) It is also important that there be some easily definable criterion for convergence of different estimators. For multiple series in general dimension, some elementary consideration of efficiency is crucial. We present below a summary of those methods that we have found useful for our multidimensional low-concentration series. The reader is referred to the above reviews for a general summary, and to the discussion of analysis methods for percolation problems in Section 3 of ref. 12 for details of our approach.

We have invoked a combination of powerful methods of series analysis which utilize a graphical approach.[12–15] The graphical approach greatly increases our ability to scan efficiently over many trial threshold values. These methods make allowance for the effect of nonconfluent corrections to scaling. Neglect of these effects led to serious discrepancies between the results of series expansion analyses and renormalization group calculations in the past. The analyses involve preliminary transforms to eliminate the interference that analytic or confluent correction terms may have on the dominant exponent and threshold values. Padé approximants are then obtained for the transformed series and these are plotted for different values of the critical fugacity, temperature, or threshold.

We assume that the series we wish to study, denoted by $H(p)$ in general, has the form for most dimensions of

$$H(p) = A(p_c - p)^{-h}[1 + a(p_c - p)^{\Delta_1} + b(p_c - p) + \cdots] \tag{4}$$

where h is the critical exponent that we wish to determine. At the upper

critical dimension there may be logarithmic corrections and these entail fitting to the form

$$H(p) = (p_c - p)^{-h} |\log(p_c - p)|^{\theta} \tag{5}$$

We use two complementary approaches, both essentially based on threshold-biased Padé approximants to transformed series (threshold-biased means that the estimated value of the critical exponent depends significantly on the value of the threshold p_c). One is to scan over a wide range of different trial thresholds and select that which exhibits optimal convergence. Our alternative approach, which avoids such a scan and is based on an old method[16] (see also ref. 15), which involves term-by-term dividing two series with the same critical threshold and then studying the "divided" series. If we begin with two series expansions $Y = \sum_{j=0,n} y_j p^j$ and $Z = \sum_{j=0,n} z_j p^j$, then we shall denote the term-by-term divided series $\sum_{j=0,n} (y_j/z_j) p^j$, by $Y \div Z$. This divided series should have critical behavior with a threshold at $p = 1$ and a dominant critical exponent equal to the difference between the exponents of the two original series plus 1. The division is expected to introduce and analytic correction to scaling [i.e., $\Delta_1 = 1$ in Eq. (4)]. If this correction has a large enough amplitude, it could provide a nice convergence region for the evaluation of the dominant exponent. Hopefully, this analytic correction is sufficient to swamp the non-analytic correction of the individual series which is still present. This method avoids the problems associated with uncertainties in p_c, but convergence is poorer owing to competing effects of the two corrections. One possible way to obtain exponents from a single series $H(p)$ when we are uncertain of the exact threshold is to utilize the above approach with series Y being $[H(p)]^2$ and series Z being $H(p)$ itself. We call the resultant series, which has a critical exponent of $h+1$, a "self-divided" series, and denote it by H^{sd}.

For both approaches we use two different algorithms, denoted by M1 and M2, for cases without logarithmic corrections. In M1,[17] we study the logarithmic derivative of

$$B(p) = hH(p) - (p_c - p)\frac{dH(p)}{dp} \tag{6}$$

which has a pole at p_c with residue $-h + \Delta_1$. For a given value of p_c we obtain graphs of Δ_1 versus input h for all Padé approximants, and we choose the triplet p_c, h, Δ_1 where all Padés converge to the same point. In the M2 method,[13,14,17] we first transform the series in p into series in the variable y, where

$$y = 1 - (1 - p/p_c)^{\Delta_1}$$

and then take Padé approximants to

$$G(y) = \Delta_1 (y-1) \frac{d}{dy} \log[H(p)] \tag{7}$$

which should converge to $-h$. Here we plot graphs of h versus the input Δ_1 for different values of p_c and choose again the triplet p_c, h, Δ_1, where all Padés converge to the same point. When $\Delta_1 = 1.0$ this method reduces[14] to the usual $d$log Padé method with threshold bias.

The analysis of the logarithmic form involves writing $\theta = zh$ and then taking Padé approximants to the series

$$g(p) = (-h)^{-1}(p_c - p) \log(p_c - p)[H(p)'/H(p) - h/(p_c - p)] \tag{8}$$

We can show that the limit of $g(p)$ as $p \to p_c$ is z. We take Padé approximants to g at the exact or most reliable estimate of p_c to obtain graphs of θ as a function of h.

We note that for both the term-by-term divided series and the temperature-biased series, it is important to use both M1 and M2 for each case. This is because for certain test[18,19] and well-behaved model[17] series the M2 analysis gives the correct dominant exponent estimate with intersection regions at the correct Δ_1 and also at resonance Δ_1/n values, where $n = 2, 3....$ Thus, it would be difficult to identify the correct Δ_1 value if we did not also have the M1 method which is resonance free.[19] We do not use M1 alone, as test series work suggests that it gives Δ_1 estimates which are less accurate than the M2 ones when Δ_1 is far from an integer. The use of two methods also eliminates the possibility that accidental spurious convergence regions will be confused with the correct results. We also note that Padé-based methods can be unduly influenced by the early terms of some series, when large analytic parts may be involved. Hence we have always studied both the series generated and several derivatives of the series when using Padé. In all cases we quote results that do not depend on the number of derivatives.

For certain problems, mainly the cases where we only had the shorter (~ 11 terms) series, it appeared that it would not be possible to resolve the confluent corrections. For these cases we have used the nonhomogeneous differential Padé approximant[20] (NHDP) in a nongraphical version. This method is especially suited to handling analytic corrections and yields reasonable results. It is especially useful when dealing with the divided series, where the analytic corrections dominate in some circumstances.[19]

Critical exponents are universal for a given problem and dimension, whereas threshold values are lattice dependent. Although we have obtained long series for hypercubic lattices only, one can use the good exponent estimates from the hypercubic series to improve the threshold estimates for

shorter series on other lattices. In addition to the evaluation of exponents and thresholds, one can study the amplitudes [A in Eq. (4)] of the series. The amplitudes themselves are not universal, but certain amplitude ratios are universal and therefore of considerable interest. The criterion of amplitude ratio is just as valid as the criterion of exponent value to distinguish between universality classes, and as we shall see in the next section, the amplitude ratio criterion is extremely useful for concentration variable systems.

A necessary condition for obtaining a universal amplitude ratio is that the ratios of the corresponding series exhibit a cancellation of the dominant critical exponents. Such ratios may be between low- and high-concentration series for the same quantity, or products of different moments of series[12,21] of, for example, the cluster size. In the former case each amplitude must be obtained independently[10] and then a ratio taken. This requires a high-precision determination of both threshold and dominant exponent, and requires long series in both concentration limits. In the latter case, series are only needed in one concentration limit, and a slight error in threshold has a much smaller effect.

There are two especially useful methods of analysis for the study of amplitude ratios of different series in the same concentration variable. One is the trivial procedure[21] of multiplying the different series and then taking Padé approximants to the resulting series, using various trial input threshold values. We find that in all cases studied the variation of ratio thoughout the entire region of uncertainty in threshold is extremely small relative to the scatter between the different Padé approximants. This insensitivity, combined with the fact that no input of exponent value is required, makes this method extremely useful, even for relatively short series. It is precisely the possibility of making this analysis that so enhances the importance of obtaining multiple moment series. In many cases of application of the above method, the corrections to scaling approximately cancel. An alternative method[15] involves term-by-term multiplication and division of the series to give a diverging series with the critical point and the exponent both equal to unity. The residuum of the pole at $p = 1$ yields a universal combination of the appropriate amplitude ratio and the exponents.

3. SPECIFIC APPLICATIONS

3.1. Geometry

Percolation and lattice animals are two of the most interesting classic geometrical models which exhibit phase transitions. For both problems general-dimensional low-concentration series were calculated to 15th order

in general dimension for hypercubic lattices.[22,12] For percolation a 16th term has been published for the mean cluster size on the square lattice,[23] and for lattice animals longer series are available for several quantities in two dimensions.[24,25] We may relate the two models by noting that the geometry of a diluted network is described by that of the infinite cluster at the percolation threshold for clusters of size smaller than the percolation correlation length ξ. For $p < p_c$, it should be described[26] by lattice animals for clusters larger than ξ. One expects that for $p < p_c$ and sufficiently large systems all universal quantities will be given by the animal values. For finite systems one expects a crossover from the percolation values to the lattice animal values. We now summarize some results for lattice animals and percolation, and discuss the nature of the crossover.

3.1.1. Lattice Animals. Let us denote by $A(n)$ the number of possible connected clusters with n bonds (or sites) embedded in a d-dimensional lattice. These clusters are called lattice animals, and they describe the statistics of dilute branched polymers. They are connected to certain lattice gauge theories[27] and can be mapped[28] onto the Yang–Lee edge singularity, which occurs at the edge of the distribution of zeros of the partition function in the complex magnetic field for classical spin models. The generating function $F(K)$ can be written as $F(K) = \sum_n A(n) K^n$, where K is the fugacity on each bond. $F(K)$ can be viewed as the free energy of the lattice animals.

Exact results for some of the critical exponents for lattice animals have been determined in up to four dimensions from several different techniques and are summarized in the introduction to ref. 22. However, since the upper critical dimension[29] is 8, this still leaves several dimensions where detailed numerical information was not available for lattice animals. The generation and analysis of 15th-order series for $F(K)$ and study of its second derivative $\chi(K) = \partial^2 F / \partial K^2$ were undertaken in order to obtain accurate estimates of the dominant exponent $\gamma_a = \gamma_H$ and of the correction exponent Δ_1.

These results for both the exponents are in excellent agreement with the third-order ε-expansion values from the Yang–Lee model.[30] This strongly suggests that the mapping between the two systems extends to the first irrelevant operator. We find $\gamma_H = 0.90 \pm 0.03$, 0.70 ± 0.04, and 0.59 ± 0.03 for $d = 5$, 6, and 7, respectively, and $\Delta_1 = 1.3 \pm 0.2$, 0.8 ± 0.2, 0.65 ± 0.15, 0.5 ± 0.2, and 0.4 ± 0.2 for $d = 3$, 4, 5, 6, and 7, respectively. The lattice-dependent critical fugacity $\lambda_c^{-1} = K_c$ values were also found to a high degree of accuracy in ref. 22. We quote $\lambda_c = 16.32 \pm 0.01$, 22.043 ± 0.0002, 27.71 ± 0.02, and 33.31 ± 0.02 for hypercubic lattices in $d = 4$, 5, 6, and 7, respectively.

3.1.2. Percolation. Early series work for the percolation problem is nicely described by Domb in Chapter 1 of ref. 3. The generating function for bond percolation has been shown[31] to be identical to the partition function for the Potts model when q, the number of states, approaches one, and it is particularly fitting to note here that the Potts model is named after R. Potts, who was a student of Prof. Domb when the "Potts" model was originated. When exact results[32] for the Potts model in 2D were first developed, their extension to the percolation limit agreed with the early series α estimate of Harris *et al.*[33] (The critical exponent α characterizes the divergence of the second derivative of the percolation "free energy" or mean number of clusters w.r.t. p.) However, the extrapolated γ estimate (γ being the exponent of the mean cluster size) appeared to contradict exponent estimates from the early series work for percolation, and this suggested to some people that hyperscaling may be violated. The reconciliation between exact results from the Potts model and the direct series expansions in 2D was eventually made by recognizing the importance of corrections to scaling. This is summarized in Chapter 17 of ref. 3.

Since the upper critical dimension for percolation[33] is 6, there have been some doubts (see the discussion in ref. 21, p. 3633) over the extension of the validity of the ε expansion down to 2D. The exponent estimates from the third-order expansion are not far from the exact results in 2D, but they do not give decisive proof either way. The amplitude ratios between low- and high-concentration series were also most problematic for percolation, since they disagreed with simulation and ε-expansion[34] results in 2D. To shed light on these questions, we studied the moments $\Gamma_j(p)$ of the percolation cluster size distribution, which are defined to be $\Gamma_j(p) = [\sum_\Gamma W(\Gamma)\, n(\Gamma)^j]_p$, with $n(\Gamma)$ the number of sites in the cluster Γ. They are believed to behave as

$$\Gamma_j(p) = A_j(p_c - p)^{-\gamma_j}[1 + a_j(p_c - p)^{\Delta_1} + \cdots] \tag{9}$$

where $\gamma_j = \gamma + (j-2)\Delta$. The gap exponent Δ is equal to $\gamma + \beta$, where β is the critical exponent of the percolation "order parameter," known as the percolation probability. These moments were intially calculated to 11th order,[21] and have recently been extended to 15 terms.[12]

To complement the series results, ε-expansion calculations for general dimension and exact results in one dimension and on "infinite"-dimensional Cayley trees have been obtained[21] for the amplitude ratios wherever possible. Excellent agreement has been obtained for all points of overlap. The 11th-order series already exhibited this agreement for the amplitude ratios right down to 2D,[21] and the longer series and alternate analysis methods applied in ref. 12 confirmed this (see Table VI of ref. 12.)

The availability of series for several moments enables the determination of two different critical exponents for each dimension. This possibility is of particular interest for percolation, where one outstanding problem in recent years has been the accurate determination of the 3D threshold and exponent values. In particular, there has been a lot of interest in the determination of the sign of the exponent η $[=2-d\gamma/(2\beta+\gamma)]$. This aspect was part of the motivation for the generation of the 15-term series.

In parallel with our latest 15th-order series, extension of both low- and high-concentration series for both the sc and bcc lattices was undertaken by Sykes and Wilkinson.[35] The only overlap is in one of the low-concentration 14th-order series on the sc lattice. Both enumerations agree, providing a powerful check on both derivations. From the series of refs. 12 and 35, threshold values of 0.2488 ± 0.0002 and 0.18025 ± 0.00015 are found for the three-dimensional bond problem on the simple cubic and body-centered cubic lattices, respectively, and 0.16005 ± 0.00015 and 0.11819 ± 0.00004 for the hypercubic bond problem in four and five dimensions, respectively. The direct exponent estimates are $\gamma = 1.805 \pm 0.02$, 1.435 ± 0.015, and 1.185 ± 0.005 and $\beta = 0.405 \pm 0.025$, 0.639 ± 0.020, and 0.835 ± 00.005 in three, four, and five dimensions, respectively. The critical exponent and threshold values in 3D are in excellent agreement with the most recent simulation results,[36] and indicate that η is negative for 3D. From the longer series outstanding agreement was also obtained with ε-expansion results for the dominant and correction exponent values in higher dimensions (see Table I in ref. 12).

3.1.3. Crossover from Percolation to Lattice Animals. In order to study the lattice animal-to-percolation crossover, a negative field can be introduced[37] into the definition of the percolation susceptibilities,

$$\chi_k(p, h) = \sum_{\Gamma} W(\Gamma)\, n(\Gamma)^k e^{-n(\Gamma)h} \tag{10}$$

11th-order series were developed for the first few moments. The effective gap exponent was determined from the term-by-term division method[15,16] with NHDP approximants. A rapid crossover was observed[37] from the percolation value ($h=0$) to the animal value of unity, over a range of $h \leqslant 0.03$. A similar crossover was observed in the amplitude ratios. The dependence of nonuniversal quantities on p can be determined by the analysis of term-by-term divided series at an h-dependent *critical point*. For example, the perimeter ratio, which is defined to be the ratio of the average numbers of perimeter sites to cluster sites in the whole range between $p=0$ and $p=p_c$, was studied. It was observed that this ratio changes over continuously from its percolation value of $(1-p_c)/p_c$ at $p=p_c$ to its animal value at $p=0$.

3.2. Resistor Networks

In addition to the study of the *geometry* of diluted networks, it is of considerable importance to elucidate their transport properties. For two transport questions that are of special interest, 13th-order low-concentration series have been obtained via the "brute-force" method, for general hypercubic lattices. The first problem concerns the accurate measurement of the conductivity exponent[38–41] t, which characterizes the conductivity in the case where we place a unit resistance on each bond. An accurate value of t is important for testing the validity of the Alexander–Orbach scaling conjecture[42] and in order to use this exponent in different applications. The exponent t can be calculated via scaling results from the resistive susceptibility.[38] The resistive susceptibilty of a resistor network is defined to be $\chi_R^{(k)} = [\sum_j v_{ij} R_{ij}^k]_p$, where R_{ij} is the resistance between sites i and j. We denote the critical exponent of the kth moment of the resistive susceptibility by $\gamma_R^{(k)}$ and its dominant amplitude by $A_R^{(k)}$. From scaling one expects[38] $\gamma_R^{(k)} = \gamma + k\zeta_R$ (where ζ_R is defined to be the critical exponent of the average resistance between two connected points) and $t = \zeta_R + (d-2)\nu$, thereby giving an estimate of t. The exponent ν is the critical exponent of the percolation correlation length. For the specific case of the square lattice, 16 terms of the resistive susceptibility have been found by Essam and Bhatti.[43] We discuss below some conclusions from previously unpublished analyses of the resistive susceptibility series. The second special transport question is that of the nature of the current distribution in resistor networks.[44] To resolve this question we studied the moments of the logarithms of the currents via 13th-order series.[45] Some other transport problems that we have studied with low-concentration series to 11th order are the full resistance distribution,[46] nonlinear resistor networks,[47] and diffusion on percolating clusters.[48]

3.2.1. Linear Resistance. The evaluation of the critical exponent t has been the focus of considerable attention over the last 10 years. Unlike the static percolation exponents, there are no exact results in 2D, and there has been a fair amount of disagreement among estimates obtained via series, simulation, and experiment. Series for $\chi_R = \chi_R^{(1)}$ and for the conductive susceptibilty χ_C (which has the critical exponent $\gamma_C = \gamma - \zeta_R$) were first developed by Fisch and Harris[38] to 10th order in 1978. This work is the basis for the application of the series approach to transport problems.

The resulting series were reanalyzed using the methods discussed in Section 2 by Alder[39] in 1985. In this reanalysis the results were biased to the best available threshold (p_c), ν and correction to scaling estimates, and the assumption was made that Δ_1 is the same as for usual percolation. The

estimates in dimensions above three were not greatly affected by the different analysis. In 3D the central t estimate was raised from 1.95 to 2.04, but the error bounds still overlapped. In 2D the analysis of the ref. 38 series reduced the t value from 1.43 to 1.36 [from $\zeta_R = (\gamma_R - \gamma_C)/2$] or to 1.31 (from $\zeta_R = \gamma_R - \gamma$). From the third way to estimate t (using $\zeta_R = \gamma - \gamma_C$), one obtains $t = 1.4$, but it can be argued[39] that the estimate of γ_C was less reliable.

With their longer 2D series Essam and Bhatti[43] found $\gamma_R = 3.65 \pm 0.02$ and $\gamma_C = 1.1 \pm 0.1$, with similar analysis methods. This leads to further reduction of the central t estimate to 1.26 (from $\zeta_R = \gamma_R - \gamma$), $t = 1.28$ (from $\zeta_R = (\gamma_R - \gamma_C)/2$), or $t = 1.29$ (from $\zeta_R = \gamma - \gamma_C$). These results are potentially problematic, since the exact $\gamma = 1.238$ does not sit midway between the γ_R and γ_C estimates, contrary to the scaling predictions.[38]

There are at least three possible ways to reconcile scaling with these measurements: (i) The γ_C estimate is indeed less reliable. Then we must quote $t = 1.26$, in significant disagreement with simulations,[49-51] which measure $t = 1.2993 \pm 0.0020$.[51] (ii) The γ_R estimate is less reliable, giving $t = 1.29$, closer to the simulation value. (iii) χ_R and χ_C do not have the same nonanalytic corrections to scaling as do the thermal quantities. If we do not know what the correction to scaling is, then we can consider the divided series $\chi_R \div \chi_C$, in the hope that the induced analytic correction will overide the unknown nonanalytic corrections. This analysis gives[41] $t \approx 1.27$ if we assume the correction to scaling for usual percolation is not swamped by the analytic term, and 1.23 with an analytic correction. In both cases only M2 gave convergent results. The severe degradation of convergence seen here could be indicative of a significant nondivergent term and therefore we explicitly quote the results of the analysis of the derivatives. The first derivative of the divided series gives $t = 1.275 \pm 0.050$, and the second $t = 1.270 \pm 0.050$ from M2, independent of the correction assumptions. We obtain convergent results from M1 with the second derivative only and quote $t = 1.29 \pm 0.02$ for this case. The other possibility is that the series may have logaritmic corrections. This last possibility can be explored by fitting to the form of Eq. (5) for various trial θ values. The best convergence is for small negative θ; for example, for $\theta = 0$, $\gamma_R = 3.66 \pm 0.02$ and $\gamma_C = 1.01 \pm 0.02$; for $\theta = -0.125$, $\gamma_R = 3.68 \pm 0.02$ and $\gamma_C = 1.03 \pm 0.02$; and for $\theta = -0.200$, $\gamma_R = 3.70 \pm 0.02$ and $\gamma_C = 1.07 \pm 0.02$; giving $t = 1.32$, 1.33, and 1.34 from $(\gamma_R - \gamma_C)/2$ for $\theta = 0$, -0.125, and -0.2, respectively. Centering of γ occurs around $\theta = -0.2$.

There has recently been renewed interest in the estimate of t in three dimensions, and so we decided to calculate the moments of χ_R to 13th order in general dimension. These series have not yet been published, and

we hope to extend them to 15th order with the NFE formalism in the future. The analysis used the new threshold estimates from ref. 12. We measure $\chi_R = 2.95 \pm 0.05$, 2.475 ± 0.05, and 2.21 ± 0.02 for $d = 3, 4$, and 5 dimensions, respectively. We present the M1 and M2 analyses of the 4D series in Fig. 1. From this figure and similar ones for other dimensions it is clear that the assumption that χ_R has the same correction to scaling as the usual percolation susceptibility is correct for $d = 3, 4$, and 5. Using our new γ and the new scaling results for the other exponents,[12] we find that t is equal to 2.02 ± 0.05, 2.40 ± 0.03, and 2.74 ± 0.03 for $d = 3, 4$, and 5, respectively. (The central estimates were 2.017, 2.396, and 2.738, respectively. The error bars quoted above reflect the maximal range of values one obtains using the maximal error ranges of the measured γ_R and the exponents in Table I of ref. 12.) The higher-dimension results can be compared with refs. 52 and 53 and earlier results quoted in Table 2 of ref. 39.

3.2.2. The Resistance Distribution. So far, we have only discussed determination of the exponents characterizing the resistance moments. However, the full distribution was determined to order ε by an ε-expansion[46] based on the work of ref. 54. In order to check these predictions, the universal quantities

$$S_{ij/kl} \equiv \frac{A_R^{(i)} A_R^{(j)} \Gamma(\gamma_R^{(k)}) \Gamma(\gamma_R^{(l)})}{A_R^{(k)} A_R^{(l)} \Gamma(\gamma_R^{(i)} \Gamma(\gamma_R^{(j)})} \tag{11}$$

have been estimated[46] by the method of ref. 15. This analysis gave excellent agreement between the series results and the ε-expansion predictions (see Table II of ref. 46).

3.2.3. Nonlinear Resistance. We next discuss the behavior of a network of nonlinear resistors, each of which obeys the generalized Ohm's law[47,55]

$$V = r|I|^{\alpha} \operatorname{sign}(I) \tag{12}$$

where V is the voltage across the resistor, I is the current, and r is the nonlinear resistance. In analogy with the linear case, one can define the nonlinear resistive susceptibility by $\chi_R(\alpha) = [\sum_j v_{ij} R_{ij}(\alpha)]_p$, where $R_{ij}(\alpha)$ is the nonlinear resistance between sites i and j. This definition is easily generalized for higher moments of the resistance, with the dominant exponent of the kth moment being denoted in general by $\zeta_k(\alpha)$ and that for $k = 2$ by $\zeta(\alpha)$ for convenience below. The exponents $\tilde{\zeta}(\alpha) \equiv \zeta(\alpha)/\nu$ were predicted[47] to reduce to certain geometrical exponents for particular values of α: $\tilde{\zeta}(\alpha \to \infty) \to 1/\nu$, $\tilde{\zeta}(\alpha = 1) = \tilde{\zeta}_R$, $\tilde{\zeta}(\alpha \to 0^+) = \tilde{\zeta}_{\min}$, $\tilde{\zeta}(\alpha \to 0^-) =$

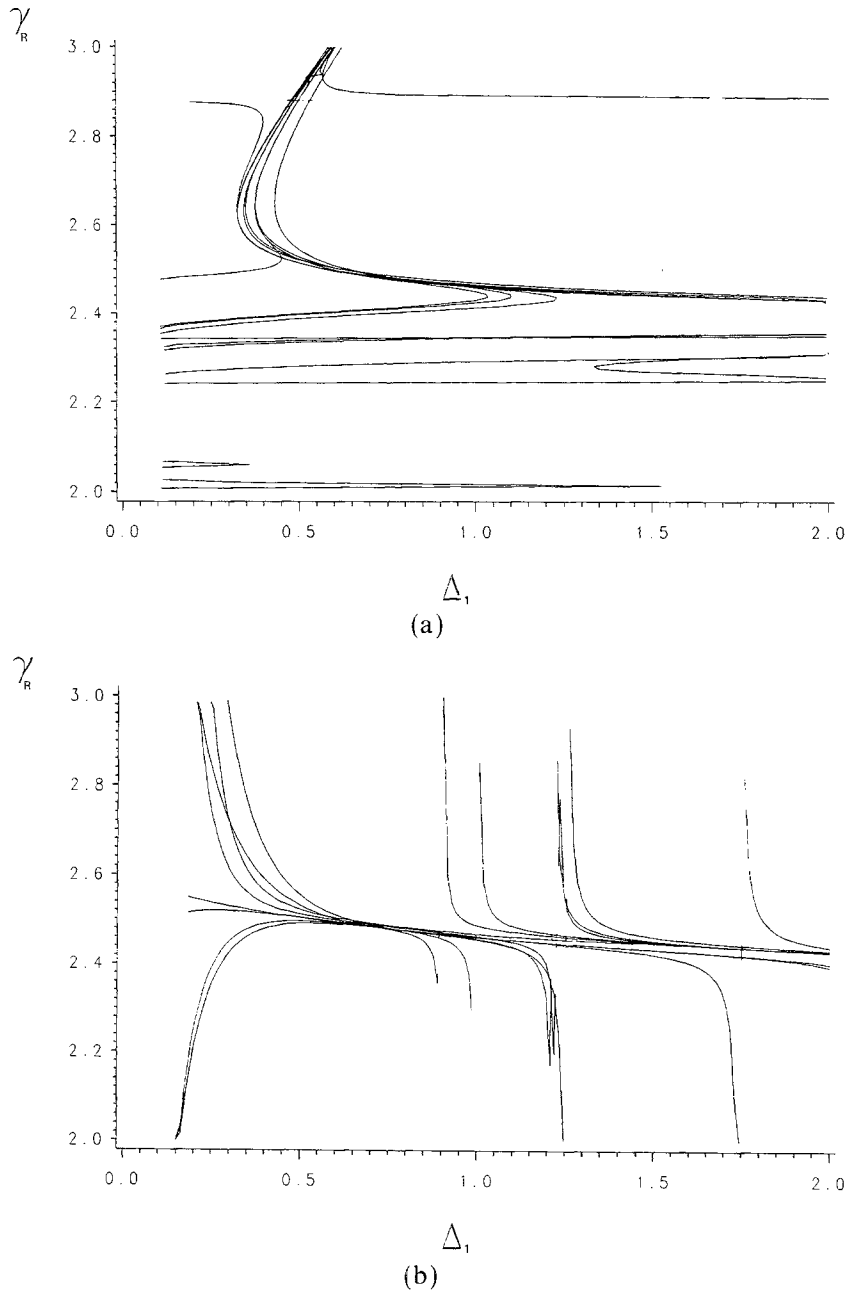

Fig. 1. Graph of different Padé approximants to (a) Δ_1 as a function of γ_R from M1, (b) γ_R as a function of Δ_1 from M2, at $p_c = 0.16005$ for the hypercubic lattice in 4D.

$\tilde{\zeta}_{\max}$, and $\tilde{\zeta}(\alpha=-1)=D_B$, where D_B is the fractal dimension of the backbone of the infinite cluster, and $\tilde{\zeta}_{\min}$ and $\tilde{\zeta}_{\max}$ characterize the scaling of the minimal and maximal self-avoiding paths, respectively. Series for $\chi_R(\alpha)$ have been constructed to 11th order in general dimension and analyzed using the NHDP method. For positive α the series were well behaved, while as α becomes more negative, the analysis becomes harder and no reliable results could be obtained for $\alpha < -1$. The resulting exponents $\zeta(\alpha)$ (for $\alpha > -1$) change continuously between the above predicted values, agreeing with previously obtained estimates of these exponents. In the whole range $-1 < \alpha < \infty$, $\zeta(\alpha)$ was very well approximated by the function

$$\zeta(\alpha) = 1 + \ln[1 + a(1 + b^{-1/\alpha})^{-c\alpha}] \tag{13}$$

where a, b, and c are fixed by the values of $\zeta(\alpha)$ for $\alpha = -1$, 0^+, and 1. These results confirm the predictions of ref. 47, and show that the nonlinear model, in addition to describing actual physical components, combines several geometrical problems, leads to inequalities between their seemingly unrelated corresponding exponents, and allows the construction of approximants for these exponents.

3.2.4. Diffusion on Percolating Clusters. Another matter of considerable interest is the question of diffusion on a percolating network, which can be related to the conductivity by following de Gennes' proposal[56] on the "ant in the labyrinth." To this aim, one can study the approach of $P_{ii}(t)$, the probability to start at site i at $t=0$ and return to it at time t, to its equilibrium value. Let us define the function[48]

$$F_{\mathrm{av}}(t) = \left[\sum_i (P_{ii}(t) - P_{ii}(\infty)) \right]_p \tag{14}$$

and study its moments through the diffusional susceptibilities

$$\chi_k(p) = \frac{1}{(k-1)!} \int_0^\infty dt\, t^{k-1} F_{\mathrm{av}}(t), \qquad k \geqslant 1 \tag{15}$$

Using the Einstein relation and scaling, the χ_k were predicted to diverge with exponents $k\Delta_\tau - \beta$, with $\Delta_\tau = \gamma + \beta + \zeta_R$, without referring to the actual diffusion mechanism. Two such processes[57] were mainly used in the literature: the blind ant, which attempts to hop in all directions with equal probability and remains in its place if the chosen bond is vacant, and the myopic ant, which chooses randomly one of the available directions. Exact relations have been obtained between the diffusional susceptibilities for these two ants and resistance correlations. To check these relations,

series for the diffusional susceptibilities [Eq. (15)] were constructed both directly and by the derived relations with the resistance correlations (which are easier to construct computerwise, since they involve matrix inversion rather than matrix diagonalization in the direct computation). The two approaches led to identical series. Analysis of the series for the blind ant gave results for Δ_τ which were consistent with the relation $\Delta_\tau = \gamma + \beta + \zeta_R$. The myopic ant estimates for the exponents agree with the blind ant ones, within their error bars. In order to have a more severe check on universality, the amplitude ratios for the two ants were compared (see Table III of ref. 48) and found to be in excellent agreement with each other, confirming the belief that the two ants belong to the same universality class. Indications were observed, however, that the myopic ant has larger corrections to scaling. These results are also consistent with the above mapping between the diffusional susceptibilities and the resistance correlations.

3.2.5. Current Distribution. In addition to the resistive properties of the network, one may study[44] the current distribution in the bonds of the network that is induced when a unit current is injected at point j and removed at point k. This distribution can be characterized by its moments[58,59] $M_q(j,k) \equiv \sum_b i_b^{2q}$, where the sum is over all bonds and i_b is the current at bond b. The zeroth moment is just the number of backbone bonds, the second moment is the resistance between points j and k, while the 4th moment is related to the resistance fluctuations. For $q \to \infty$ only the singly connected bonds that carry unit current survive in the sum. In ref. 44 series were constructed and analyzed for the generalized susceptibilities

$$\chi^{(q)}(p) = \left[\sum_k v_{jk} M_q(j,k) \right]_p \tag{16}$$

which have a dominant exponent denoted by $\gamma + \psi(q)$. From the above relations one has $(\tilde{\psi} = \psi/\nu)$ $\tilde{\psi}(q=0) = D_B$, $\tilde{\psi}(q=1) = \zeta_R$, and $\tilde{\psi}(q \to \infty) = 1/\nu$, where $1/\nu$ is the fractal dimension of the singly connected bonds.[60] The results indeed indicate that $\tilde{\psi}(q)$ changes continuously between the above predicted values and is very well approximated by the functions[44]

$$\psi(q) = 1 + (\nu D_B - 1)^{1-q} (\zeta_R - 1)^q \tag{17}$$

$$\psi(q) = 1 + a/(q+1)(q+b) \tag{18}$$

For the negative moments we observed[44] that the critical threshold is changing continuously as a function of q. This is due to the fact that these

moments are dominated by exponentially large contributions from exponentially rare realizations (a situation very similar to that occurring in self-avoiding walks on diluted networks). The fact that the negative moments are dominated by the tail of the current distribution demonstrates that the whole distribution cannot be characterized by the leading scaling behavior of the positive moments.[61] The physical relevance of the negative moments was pointed out by Redner *et al.*[62]

3.2.6. Logarithms of the Moments. The fact that $\tilde{\psi}(q)$ does not exhibit a constant gap led some groups[59] to the conjecture that the distribution of i_b may be log-normal, i.e., that the moments of $\ln i_b$, $\mu_q = \sum_b |\ln i_b|^q$, may have a constant gap exponent. To check this conjecture, we undertook[45] a series study of μ_q.

In one dimension it has been shown[45] that

$$\mu_q = |\ln(1-p)|^{cq}/(1-p)^{\gamma} \tag{19}$$

exactly, with $c = \gamma = 1$, for both positive and negative moments.

In order to study the suitability of the functional form of Eq. (19) for higher dimensions, we generated 13th-order series for several moments in general dimension. The series were analyzed by methods discussed in Section 3 and also by several new methods especially tailored to the problem at hand. Our methods duplicated the results for one dimension, although for the negative moments we found that series of over 20 terms were needed for accuracy at $q \approx -5$. The results of the analysis for $d > 1$ were consistent with the form of Eq. (19) for $0 < q < 6$, but we found c values that were a little larger than 1.0 in 2D and 3D. For other q values we do not see a constant gap; this may be due to the shortness of the series or to real deviations from a log-normal distribution. A detailed discussion will be given in ref. 45.

3.3. Spin Problems

Another group of problems that are included in the scope of this review are those where the dilution of a spin system leads to some interesting new type of behavior. For some of these systems a two- ($1/T$ and p) or three- ($1/T$, p, and H—magnetic field) variable series expansion can be made, but we shall concentrate below on aspects relating to the p expansion or the crossover to this limit. Models of this type for which long low-concentration general-dimension expansions have been used include the dilute Ising model (DIM),[63] the dilute Edwards–Anderson Ising spin glass at zero temperature (T0DSG),[19] the dilute random field Ising model

(RFIM),[64,65] the dilute antiferromagnet in a uniform field (DAFF),[64,65] and the dilute quantum spin-1/2 Heisenberg ferromagnet.[66] The T0DSG series use the NFE formalism and therefore extend to 15th order, the others are 11th order, excepting the last, which is still in the process of generation and may reach further. In some of these problems the threshold remains identical to the percolation threshold, in others it varies quite considerably. The exponents of the transition likewise remain percolation-like or differ.

3.3.1. Dilute Ising Model. The dilute Ising model is defined by the Hamiltonian

$$H = -\sum_{ij} J_{ij} S_i S_j \tag{20}$$

where the sum is over nearest neighbors, S_i is the local Ising spin at site i, and J_{ij} are random variables with a binary distribution, $P(J_{ij}) = p\delta(J_{ij} - J) + (1-p)\,\delta(J_{ij})$, with $J > 0$. Near the percolation threshold the magnetic susceptibility can be written in the scaling form

$$\chi(p, T) = A(p_c - p)^{-\gamma} F(w(p_c - p)^{-\theta}) \tag{21}$$

where $w = \exp(-2J/kT)$ and θ, the crossover exponent, is equal to unity (see, e.g., ref. 67). We studied[63] the crossover function by expanding it in powers of w,

$$\chi(p, T) = \sum_{n=0}^{\infty} \chi_n(p) w^n \tag{22}$$

General-dimension series for $\chi_n(p)$ have been constructed to 11th order. From their analysis, we found that the gap exponent, which is equal to θ, is indeed unity in all dimensions. We also found good agreement between amplitude ratios involving the χ_n and newly derived ε-expansion estimates.[63]

3.3.2. Dilute Zero-Temperature Spin Glass. We use[19] 15th-order series expansions to study the critical behavior of the dilute Ising spin glass at zero temperature (T0DSG) as a function of the concentration of occupied bonds p. In the Ising spin glass, nearest-neighbor exchange interactions take the values $\pm J$ randomly; in the T0DSG they assume the

values $+J, 0, -J$ with probabilities $p/2, 1-p$, and $p/2$, respectively. We have calculated series for the Edwards–Anderson spin-glass susceptibility ($\chi_{EA} = \sum_j [\langle S_i S_j \rangle]_c$, where $\langle \cdot \rangle$ denotes the thermal average for a given quenched configuration and $[\cdot]_c$ denotes the configurational average over the exchange interactions) for the T0DSG for hypercubic lattices in general dimension.

Analysis of the T0DSG series gives[19] the first conclusive numerical evidence that p_{sg} (the critical concentration of bonds below which no long-range spin glass order occurs) is above the percolation threshold p_c. This result holds in all dimensions $d \geqslant 2$. We observe strong indications that the critical exponent of χ_{EA} is distinct from that of percolation. Our results are consistent with the scenario that there is a crossover from percolation exponents to $q = 1/2$ state Potts exponents to those of the thermal spin glass and this crossover becomes more pronounced as the length of the series increases.

3.2.3. Dilute Spin-1/2 Quantum Heisenberg Antiferromagnet. A recent significant step forward in the development of our formalism is its application to models where the spins have a quantum nature. Series for the ground-state energy and staggered magnetization of the dilute spin-1/2 quantum Heisenberg model in general dimension have been obtained to date[66] through to 9th order and are presently being extended. With our present graph tables we have the potential to obtain 13th-order series for quantum problems, but limitations of computer resources for the necessary matrix diagonalizations may inhibit this potential.

3.2.4. Dilute Antiferromagnet in a Field and Random Field Ising Model. Other dilute systems of interest are the RFIM and the DAFF.[64,65] By scaling arguments they should have the same critical exponents for $d > 1$, this exponent being identical with $(\gamma - \beta)/2$ of usual percolation.[64] 11th-order series have been studied for the susceptibility of these models using both the NHDP and the graphical methods M1 and M2. The former method initially suggested[64] that while the exponents of the two systems appeared to agree for $d = 4$ and 5, they differed from each other at $d = 2$ and 3. A reanalysis of the series was made in ref. 65 using the methods that allowed for the effects of corrections to scaling and then current threshold, γ and β values. This reanalysis showed that it was important to consider corrections to scaling, and a further comparison with the most recent scaling estimates[12] shows that the exponent estimates are consistent with each other and the scaling estimates for $d > 2$. In 2D we find γ_{DAFF} agrees with the scaling result, but γ_{RFIM} is a little low.

3.4. Other Problems

Several other problems on diluted lattices that have been investigated by low-concentration series include self-avoiding walks on diluted lattices[68] and quantum percolation.[69]

3.4.1. Self-Avoiding Walks on Percolation Clusters. It is well known[70] that the statistics of long self-avoiding walks (SAWs) on an undiluted lattice can be obtained in the $n \to 0$ limit of the n-state Heisenberg-like model. Hence, it can be characterized by two critical exponents, such as the exponent γ_{saw} that describes the scaling of the number of N-step SAWs with N, and the exponent ν_{saw} describing the scaling of the average end-to-end distance with N. It is easy to show that in the presence of dilution, γ_{saw} does not change.[71] It is also expected that for $p > p_c$, $\nu_{\text{saw}}(p)$ is still given by the pure system value. However, it is not clear what happens at $p = p_c$. Recently there have been some suggestions[72] that the exponent $\nu_{\text{saw}}(p = p_c)$ is still given by the pure system value. Real-space and momentum-space renormalization group results[68] run counter to this suggestion. In order to check this, 11th-order series were constructed for

$$\bar{N}(K) = \left[\sum_j v_{ij} \bar{N}_{ij}(K) \right]_p \sim (p_c - p)^{-\gamma - \phi} \tag{23}$$

where $\bar{N}_{ij}(K)$ is the number of steps averaged over all SAWs between sites i and j, when each step is weighted by a fugacity K. The ϕ varies from $\zeta_{\min}$ for small K to $\zeta_{\max}$ for large K, supporting the real-space renormalization-group results. According to the latter results, there is a special value of K, K_0, which describes the average SAW. The analysis at this value leads to $\nu_{\text{saw}}(p = p_c) \equiv \nu/\phi = 0.76 \pm 0.08$, 0.67 ± 0.04, 0.63 ± 0.02, and 0.54 ± 0.02 for $d = 2$, 3, 4, and 5, respectively. These values exclude the pure lattice values for $d > 2$, further substantiating our predictions.

3.4.2. Quantum Percolation and Localization. The quantum percolation model (QPM) is defined by the Hamiltonian

$$H = \sum_{\langle ij \rangle} V_{ij} |i\rangle\langle j| + \text{h.c.} \tag{24}$$

where $|i\rangle$ represents a wave function localized near site i and V_{ij}, the nearest-neighbor hopping matrix elements, are taken from a binary distribution $P(V_{ij}) = p\delta(V_{ij} - 1) + (1 - p)\,\delta(V_{ij})$. This model may

describe granular materials and mixtures of metal and insulator at low temperatures.

First we constructed series for the quantity $\chi(p)$ related to the inverse participation ratio. We set[69]

$$\chi(p) = \left[\sum_i \left(\sum_E |\psi_E(i)|^4 \right)^{-1} \right]_p \tag{25}$$

where $\psi_E(i)$ is the amplitude of the wave function ψ_E at site i. The $\chi(p)$ should diverge at p_q, where a finite fraction of the states becomes extended. The analysis led to $p_q \simeq 0.33 \pm 0.06$, 0.20 ± 0.04, and 0.17 ± 0.02 in 3, 4, and 5 dimensions. In $d=2$ there is a trace of a singular behavior in the range $p = 0.6$–0.8.

In order to obtain more accurate results, we constructed 13th-order series for the average transmission coefficient,

$$T(p, E) = \left[\sum_i T_{ij}(E) \right]_p \tag{26}$$

where $T_{ij}(E)$ is the transmission coefficient between points i and j; we attach one-dimensional perfect leads to points i and j, insert an incoming wave with energy E on one lead, and, using the QPM, calculate the amplitude of the transmitted wave as a function of E. The series (26) should diverge once the localization length diverges, i.e., at the delocalization transition. The analysis of these series leads to the critical thresholds $p_q(E=0.05) = 0.32 \pm 0.04$, 0.22 ± 0.02, and 0.18 ± 0.02 in 3, 4, and 5 dimensions, respectively. Our results from T are quite close to those found from $\chi(p)$, but are more accurate. The results of the series for T in 2D are much more definitive than those for $\chi(p)$ of previous works, and lead to $p_q = 0.60 \pm 0.04$. Further checks showed that $T(p)$ has a *power law* singularity at $p = p_q$ in 2D), while the one-parameter scaling theory[73] predicts an essential singularity at $p = 1$.

There are three scenarios to explain our results: (a) There is a transition in 2D between exponential and power law localization. This may not contradict the scaling theory. (b) The transition may be peculiar to the kind of disorder discussed in our model. (c) The one-parameter scaling theory fails, at least in two dimensions.

4. CONCLUSIONS

We have given some examples of the power of the series expansion approach to problems in randomly diluted systems. There are many direc-

tions for future work with series expansions. These include the extension of the NFE graph tables to higher order, this project being quite within the range of current computer capability. Another future direction is the generation of long series for multiple moments in two variables in general dimension. For some interesting problems of this type rather a lot of computer time will be needed in order to use all the graphs currently tabulated. However, there may be a possibility of vectorization and parallelization of part of the algorithms, and future developments in computers will be very useful here.

A final reminder is given that this review has been extremely selective in the topics covered. Related topics that we chose not to discuss for reasons of space include the series generation method known as the "star-graph" expansion. A discussion of this efficient, but not always applicable approach can be found in the review by Fisher and Singh.[7] Related models for which low-concentration series have been developed in several dimensions include directed percolation (recent references to this system include Essam *et al.*[74] for 2D and Adler *et al.*[75] for higher dimensions) and the directed animal enumerations of Duarte.[76] Many low-concentration series have been developed in 2D only. Such calculations include series for bond bending and central force percolation[77] and for bootstrap percolation[78] and many different lattice animal variants.

ACKNOWLEDGMENTS

We thank Prof. C. Domb for his role is developing such a useful method, and for the personal encouragement he has given all of us since his arrival in Israel. We thank the various people who have collaborated on some of the work reported here, especially Rafi Blumenfeld. We also thank the authors of the various Monte Carlo simulations who sent us prepublication estimates of their results, and especially Dietrich Stauffer, whose constant push encouraged many of the data reanalyses discussed above. The assistance of the Technion Computer Centre consultants in the manipulation of the graph data tapes is gratefully acknowledged.

This work was supported in part by grants from the Israel Academy of Sciences and Humanities and by the U. S.–Israel Binational Science Foundation. Also, A.B.H. acknowledges partial suport from the MRL program of the National Science Foundation under grant DMR 85-19059, and J.A. acknowledges support from the Technion Vice President's Research Fund and the New York Metropolitan Research Fund.

REFERENCES

1. C. Domb and M. S. Green, eds., *Phase Transitions and Critical Phenomena*, Vol. 2 (Academic, New York, 1972).
2. C. Domb and M. S. Green, eds., *Phase Transitions and Critical Phenomena*, Vol. 3 (Academic, New York, 1974).
3. G. Deutscher, R. Zallen, and J. Adler, eds., *Percolation Structures and Processes* (Adam Hilger, London, 1983).
4. J. L. Martin, in *Phase Transitions and Critical Phenomena*, Vol. 3, C. Domb and M. S. Green, eds. (Academic, New York, 1975), p. 97.
5. A. B. Harris, *Phys. Rev. B* **26**:337 (1982).
6. A. B. Harris and Y. Meir, *Phys. Rev. A* **36**:1840 (1987).
7. M. E. Fisher and R. R. P. Singh, in *Disorder in Physical Systems*, G. Grimmett and D. J. A. Welsh, eds., in press.
8. H. Gould and J. Tobochnik, *Computer Simulation Methods* (Addison-Wesley, Reading, Massachusetts, 1988).
9. D. Stauffer, *Introduction to Percolation Theory* (Taylor and Francis, London, 1985).
10. D. S. Gaunt and A. J. Guttmann, in *Phase Transitions and Critical Phenomena*, Vol. 3, C. Domb and M. S. Green, eds. (Academic, New York, 1974), p. 181.
11. A. J. Guttmann, in *Phase Transitions and Critical Phenomena*, C. Domb and J. Lebowitz, eds. (Academic, New York, to appear).
12. J. Adler, Y. Meir, A. B. Harris, and A. Aharony, *Bull. Israel Phys. Soc.* **35**:10.2 (1989), *Phys. Rev. B*, in press, and references therein.
13. J. Adler, M. Moshe, and V. Privman, *Phys. Rev. B* **26**:1411 (1982).
14. J. Adler, M. Moshe, and V. Privman, in *Percolation Structures and Processes*, G. Deutscher, R. Zallen, and J. Adler, eds. (Adam Hilger, London, 1983), p. 397.
15. Y. Meir, *J. Phys. A* **20**:L349 (1987).
16. D. L. Hunter and G. A. Baker, Jr., *Phys. Rev. B* **7**:3346 (1973).
17. J. Adler, M. Moshe, and V. Privman, *J. Phys. A* **14**:L363 (1981); see also J. Adler and I. G. Enting, *J. Phys. A* **17**:2233 (1984).
18. V. Privman, *J. Phys. A* **16**:3097 (1983).
19. L. Klein, J. Adler, A. Aharony, A. B. Harris, and Y. Meir, *Bull. Israel Phys. Soc.* **35**:10.10 (1989); *Phys. Rev. B* **40**:4824 (1989); and in preparation.
20. J. L. Gammel, in *Padé Approximants and Their Applications*, B. R. Graves-Morris, ed. (Academic, New York, 1973).
21. J. Adler, A. Aharony, Y. Meir, and A. B. Harris, *J. Phys. A* **19**:3631 (1986).
22. J. Adler, Y. Meir, A. B. Harris, A. Aharony, and J. A. M. Duarte, *Phys. Rev. B* **38**:4941 (1988).
23. D. F. Styer, M. D. Edwards, and E. A. Andrews, *J. Phys. A* **21**:L1153 (1988).
24. D. H. Redelmeier, *Discuss. Math.* **36**:191 (1981).
25. A. J. Guttmann, *J. Phys. A* **15**:1987 (1982); A. Margolina, Z. V. Djordjevic, D. Stauffer, and H. E. Stanley, *Phys. Rev. B* **28**:1652 (1983).
26. D. Stauffer, *Phys. Rep.* **54**:1 (1979).
27. J. M. Drouffe, G. Parisi, and N. Sourlas, *Nucl. Phys. B* **161**:397 (1979).
28. G. Parisi and N. Soulas, *Phys. Rev. Lett.* **46**:871 (1981); D. Dhar, *Phys. Rev. Lett.* **10**:853 (1983).
29. T. C. Lubensky and J. Issacson, *Phys. Rev. Lett.* **41**:829 (1978); **42**:410(E) (1979); *Phys. Rev. A* **20**:2130 (1979).
30. O. F. de Alcantara Bonfim, J. E. Kirkham, and A. J. McKane, *J. Phys. A: Math. Gen.* **13**:L247 (1980); **14**:2391 (1981).

31. P. W. Kasteleyn and C. M. Fortuin, *J. Phys. Soc. Jpn.* (Suppl.) **26**:11 (1969); C. M. Fortuin and P. W. Kasteleyn, *Physica* (Utrecht) **57**:536 (1972).
32. B. Nienhuis, *J. Phys. A* **15**:199 (1982); M. P. M. den Nijs, *J. Phys. A* **12**:1857 (1979); B. Nienhuis, E. K. Riedel, and M. Schick, *J. Phys. A* **13**:189 (1980); R. B. Pearson, *Phys. Rev. B* **22**:2579 (1980).
33. A. B. Harris, T. C. Lubensky, W. K. Holcomb, and C. Dasgupta, *Phys. Rev. Lett.* **35**:327, 1397E (1975), and references therein.
34. A. Aharony, *Phys. Rev. B* **22**:400 (1980).
35. M. F. Sykes and M. K. Wilkinson, *J. Phys. A* **19**:3415 (1986).
36. R. M. Ziff and G. Stell, private communication.
37. Y. Meir, A. Aharony, and A. B. Harris, *Phys. Rev. B* **39**:649 (1989).
38. R. Fisch and A. B. Harris, *Phys. Rev. B* **18**:416 (1978).
39. J. Adler, *J. Phys. A* **18**:307 (1985).
40. J. Adler, A. Aharony, A. B. Harris, and Y. Meir, unpublished.
41. J. Adler, unpublished.
42. S. Alexander and R. Orbach, *J. Phys. Lett.* (Paris) **43**:L625 (1982).
43. J. W. Essam and F. Bhatti, *J. Phys. A* **18**:3577 (1985).
44. R. Blumenfeld, Y. Meir, A. Aharony, and A. B. Harris, *Phys. Rev. B* **35**:3524 (1987).
45. R. Blumenfeld, J. Adler, Y. Meir, A. Aharony, and A. B. Harris, in preparation.
46. A. B. Harris, Y. Meir, and A. Aharony, *Phys. Rev. B*, in press.
47. R. Blumenfeld and A. Aharony, *J. Phys. A* **18**:L443 (1985); Y. Meir, R. Blumenfeld, A. Aharony, and A. B. Harris, *Phys. Rev. B* **34**:3424 (1986); Y. Meir, R. Blumenfeld, A. Aharony, and A. B. Harris, *Phys. Rev. B* **36**:3950 (1987); R. Blumenfeld, Y. Meir, A. B. Harris, and A. Aharony, *J. Phys. A* **19**:L791 (1986).
48. A. B. Harris, Y. Meir, and A. Aharony, *Phys. Rev. B* **36**:8752 (1987).
49. J. G. Zabolitsky, *Phys. Rev. B* **30**:4077 (1984); H. J. Herrmann, B. Derrida, and J. Vannimenus, *Phys. Rev. B* **30**:4080 (1984).
50. D. C. Hong, S. Havlin, H. J. Herrmann, and H. E. Stanley, *Phys. Rev. B* **30**:4083 (1984); C. J. Lobb and D. J. Frank, *Phys. Rev. B* **30**:4090 (1984).
51. J.-M. Normand, H. J. Herrmann, and M. Hajjar, *J. Stat. Phys.* **52**:441 (1988).
52. R. B. Pandey, D. Stauffer, J. G. Zabolitsky, and A. Margolina, *J. Stat. Phys.* **34**:427 (1984).
53. R. B. Pandey, D. Stauffer, and J. G. Zabolitsky, *J. Stat. Phys.* **49**:849 (1987).
54. A. B. Harris and T. C. Lubensky, *Phys. Rev. B* **23**:3591 (1981), **24**:2656 (1981).
55. S. W. Kenkel and J. P. Straley, *Phys. Rev. Lett.* **49**:767 (1982); J. P. Straley and S. W. Kenkel, *Phys. Rev. B* **29**:6299 (1984).
56. P. G. de Gennes, *Recherche* **7**:919 (1976).
57. C. D. Mitescu and J. Roussenq, in *Percolation Structure and Processes*, G. Deutscher, R. Zallen, and J. Adler, eds. (Adam, eds. (Adam Hilger, London, 1983), p. 81.
58. R. Rammal, C. Tannous, and A.-M. S. Tremblay, *Phys. Rev. A* **31**:2662 (1985).
59. L. de Arcangelis, S. Redner, and A. Coniglio, *Phys. Rev. B* **31**:4725 (1985).
60. A. Coniglio, *Phys. Rev. Lett.* **46**:250 (1981); *J. Phys. A* **15**:3829 (1982).
61. A. Aharony, R. Blumenfeld, P. Breton, B. Fourcade, A. B. Harris, Y. Meir, and A.-M. S. Tremblay, *Phys. Rev. B* **40**:7314 (1989).
62. S. Redner, J. Koplik, and D. Wilkinson, *J. Phys. A* **20**:1543 (1987).
63. D. Chomsky, Y. Meir, and A. Aharony, unpublished.
64. A. Aharony, A. B. Harris, and Y. Meir, *Phys. Rev. B* **32**:3203 (1985).
65. J. Adler, A. Aharony, Y. Meir, and A. B. Harris, *Phys. Rev. B* **34**:3469 (1986).
66. C. C. Wan, A. B. Harris, and J. Adler, unpublished.
67. M. J. Stephen and G. S. Grest, *Phys. Rev. Lett.* **10**:567 (1977).

68. Y. Meir and A. B. Harris, submitted.
69. Y. Meir, A. Aharony, and A. B. Harris, *Europhys. Letters* **10**:275 (1989).
70. P. G. de Gennes, *Phys. Lett. A* **38**:339 (1972).
71. J. Lyklema and K. Z. Kremer, *Z. Phys. B* **55**:41 (1981); A. B. Harris, *Z. Phys. B* **49**:000 (1983).
72. S. B. Lee and H. Nakanishi, *Phys. Rev. Lett.* **61**:2022 (1988); S. B. Lee, H. Nakanishi, and Y. Kim, *Phys. Rev. B* **39**:9561 (1989).
73. E. Abrahams, P. W. Anderson, D. C. Licciardello, and T. V. Ramakrishnan, *Phys. Rev. Lett.* **42**:673 (1979).
74. J. W. Essam, A. J. Guttmann, and K. De'Bell, *J. Phys. A* **21**:3185 (1988).
75. J. Adler, J. Berger, J. A. M. S. Duarte, and Y. Meir, *Phys. Rev. B* **37**:4941 (1988).
76. J. A. M. S. Duarte, *J. Phys. Lett.* (Paris) **46**:L523 (1985).
77. J. Wang, A. B. Harris, and J. Adler, in preparation.
78. M. Cox and J. W. Essam, private communication.